Substrate translocation involves specific lysine residues of the central channel of the conjugative coupling protein TrwB

Delfina Larrea,[a,1] Héctor D. de Paz,[a,2] Inmaculada Matilla,[a,3] Dolores L. Guzmán-Herrador,[a] Gorka Lasso,[b] Fernando de la Cruz,[a] Elena Cabezón,[a] Matxalen Llosa[a#]

[a] Departamento de Biología Molecular, Universidad de Cantabria, and Instituto de Biomedicina y Biotecnología de Cantabria, IBBTEC (Universidad de Cantabria, CSIC, SODERCAN), Santander, Spain

[b] Department of Biochemistry and Molecular Biophysics, Center for Computational Biology and Bioinformatics, Department of Systems Biology, Howard Hughes Medical Institute, Columbia University, New York, New York 10032, USA.

Running Head: Role of TrwB central channel in bacterial conjugation

Address correspondence to: llosam@unican.es

ORCID 0000-0002-4826-2240

[1] Present address: Department of Neurology, Columbia University Medical Center, New York, USA.

[2] Present address: Molecular Microbiology Department, University Hospital Sant Joan de Déu, Esplugues de Llobregat, Barcelona, Spain

[3] Present address: Cell Biology Unit, Children's Medical Research Institute, Westmead, Australia.

Abstract

Conjugative transfer of plasmid R388 requires the coupling protein TrwB for protein and DNA transport, but their molecular role in transport has not been deciphered. We investigated the role of residues protruding into the central channel of the TrwB hexamer by a mutational analysis. Mutations affecting lysine residues K275, K398 and K421, and residue S441, all facing the internal channel, affected transport of both DNA and the relaxase protein *in vivo*. The ATPase activity of the purified soluble variants was affected significantly in the presence of accessory protein TrwA or DNA, correlating with their behaviour *in vivo*. Alteration of residues located at the cytoplasmic or the inner membrane interface resulted in lower activity *in vivo* and *in vitro*, while variants affecting residues in the central region of the channel showed increased DNA and protein transfer efficiency, and higher ATPase activity, especially in the absence of TrwA. In fact, these variants could catalyse DNA transfer in the absence of TrwA under conditions in which the wild-type system was transfer-deficient. Our results suggest that protein and DNA molecules have the same molecular requirements for translocation by Type IV secretion systems, with residues at both ends of the TrwB channel controlling the opening-closing mechanism, while residues embedded in the channel would set the pace for substrate translocation (both protein and DNA) in concert with TrwA.

Keywords: Bacterial conjugation / Type IV secretion systems / DNA transport / molecular motors

Introduction

Bacterial conjugation is a highly efficient and promiscuous process of DNA transfer from donor to recipient bacteria, which contributes to horizontal dissemination of DNA in Gram-negative and Gram-positive bacteria (Thomas and Nielsen 2005). Conjugative coupling proteins are essential elements of the DNA transfer machinery (Christie 2016). These proteins form hexamers anchored to the inner membrane. Their ATPase activity is required for the transport of the DNA molecule as well as the protein which leads the DNA into the recipient cell (Llosa et al. 2003). Early and current models of conjugative DNA transfer propose that the DNA strand is pumped into the recipient travelling along the internal channel (ICH) of the hexamer (Llosa et al. 2002; Cabezon et al. 2015), but there is no conclusive evidence.

The conjugative apparatus involves different functional modules (Llosa and de la Cruz 2005; Cabezon et al. 2015): the protein-DNA complex responsible for substrate processing called relaxosome, and a Type IV secretion system (T4SS) for substrate secretion. The relaxosome is comprised of a DNA site, the origin of transfer (*oriT*), the relaxase, and additional relaxase accessory proteins and host factors. In Gram-negative bacteria, the T4SS is comprised of a core channel complex spanning the bacterial envelope, an extracellular pilus involved in cell-to-cell contact, and three cytoplasmic hexameric ATPases that supply the energy for pilus biogenesis and substrate transport. One of these ATPases is the Type IV coupling protein (T4CP), required to couple the relaxosome to the T4SS. To accomplish DNA transfer, the relaxase cleaves the DNA strand to be transferred and remains covalently bound to the T-strand; this nucleoprotein complex is recruited and translocated by the T4SS into the recipient cell, where the relaxase catalyzes recircularization of the DNA.

Type IV coupling proteins (T4CPs) are present in all conjugative systems, and in many Type IV secretion systems (T4SSs) involved in bacterial virulence (Gonzalez-Rivera et al. 2016). T4CPs are dispensable for pilus biogenesis but required for substrate translocation (Lai et al. 2000a; Lawley et al. 2002), probably playing a major role in substrate recruitment. Evolutionary and biochemical work supports the assumption that T4CPs have an independent origin and function from their cognate T4SS (Cabezon et al. 2012; Guglielmini et al. 2013; Larrea et al. 2013). T4CPs belonging to the VirD4-like protein family, e.g., F-TraD, RP4-TraG, R388-TrwB and *Agrobacterium tumefaciens*-VirD4 (de la Cruz et al. 2010), display low sequence identities (15-20%) but share conserved features, including a nucleotide-binding domain with Walker boxes A and B, which are essential for conjugation, and a transmembrane domain (TMD) for anchoring them to the inner membrane.

The soluble derivative of the R388 T4CP, TrwBΔN70, devoid of the TMD, is a DNA-dependent ATPase (Tato et al. 2005). ATPase activity is stimulated by the CTD of the relaxosomal protein TrwA (Tato et al. 2007), and by both double stranded DNA (dsDNA) and single stranded DNA (ssDNA) (Tato et al. 2005; Tato et al. 2007), but more specifically by G4 DNA structures (Matilla et al. 2010). The crystallographic structure of TrwBΔN70 (Gomis-Rüth et al. 2001; Gomis-Rüth et al. 2002) reveals a hexamer with a 6-fold symmetry and an ICH of approximately 20 Å in diameter. The ICH is composed of 180 surface residues (solvent accessible surface area >= 10$Å^2$), of which 114 (19 per monomer) correspond to charged residues; 48 positively charged and 66 negatively charged surface residues. Each monomer is composed of two main structural domains: the nucleotide-binding domain showing a RecA-like fold, and a small membrane-distal all-alpha domain. The TMD of TrwB plays an important role in TrwB structural integrity and oligomerization (Hormaeche et al. 2002; Hormaeche et al. 2004; de Paz et al. 2010; Vecino et al. 2011), subcellular localization

93 (Segura et al. 2014), and regulation of ATPase activity (Hormaeche et al. 2006; Vecino et al.
94 2010).

95 A coupling role for T4CPs is supported by early genetic data (Cabezón et al. 1997) and
96 evidence of protein-protein interactions with both the substrate and the T4SS. Interactions
97 with relaxosomal proteins were described for different conjugative T4CPs, both from Gram-
98 negative (Schröder et al. 2002; Llosa et al. 2003; Tato et al. 2007; Lu et al. 2008; Lang et al.
99 2011) and Gram-positive (Chen et al. 2008) plasmids. Moreover, an interaction with the
100 substrate has also been reported for *Helicobacter pylori* T4CP Cag β and its secreted
101 substrate CagA (Jurik et al. 2010). The carboxy-terminal domain (CTD) is the candidate
102 domain for substrate interaction, as suggested by structural and functional data in different
103 systems (Sastre et al. 1998; Lu et al. 2008; Whitaker et al. 2015; Whitaker et al. 2016).
104 T4CP:T4SS interactions have been reported with the T4SS core component VirB10 (Gilmour
105 et al. 2003; Llosa et al. 2003; Atmakuri et al. 2004). The T4CP-VirB10 interaction was shown
106 to be responsible for efficiency of DNA transfer (Llosa et al. 2003). VirB10 is proposed to act
107 as a regulator of the T4SS outer-membrane pore (Cascales and Christie 2004); thus, a mating
108 signal could be transmitted from the outside of the cell to the relaxosome via the T4CP-
109 VirB10 interaction (de Paz et al. 2010). While the interaction with the relaxosome is highly
110 specific for its cognate system, a single T4CP can interact functionally with several
111 conjugative T4SSs (Llosa et al. 2003) and even with T4SSs involved in bacterial virulence,
112 leading to DNA transfer into the human cells targeted by the pathogen (Fernández-González
113 et al. 2011; Schröder et al. 2011). Interestingly, it was recently shown that chimeric T4CP
114 could recruit the cognate substrates of their CTD to the cognate T4SS of their TMD,
115 emphasizing their self-sufficiency as substrate recruiters for T4SS (Whitaker et al. 2016).

In addition to the interactions with VirB10, the T4CP also interacts with the two cytoplasmic ATPases VirB4 and VirB11 (Atmakuri et al. 2004; Ripoll-Rozada et al. 2013). It has been proposed that interactions between the three cytoplasmic ATPases may be dynamic, representing alternative functional conformations of the T4SS (Ripoll-Rozada et al. 2013). In Gram-positive plasmids pLS20 and pCF10, interaction of the T4CP with the VirB4 homologue was reported (Bauer et al. 2011; Li et al. 2012a). Moreover, the ATPase activity of the T4CP TrwB is inhibited in the presence of an ATPase- defective mutant of TrwK, the VirB4 homolog in plasmid R388, which suggests that both proteins can interact with each other to form heterocomplexes (Pena et al. 2012). There is a striking structural homology between TrwB and the CTD of VirB4 homologues (Pena et al. 2012; Wallden et al. 2012), although these two ATPases are proposed to act at different steps of the conjugative process. VirB4 proteins seem to mediate pilin dislocation from the inner membrane, promoting pilus formation (Kerr and Christie 2010), whereas the T4CP would be required in subsequent processing steps to pump the plasmidic DNA through the channel (Llosa et al. 2002; Cabezon and de la Cruz 2006). This proposal is based on its DNA-dependent ATPase activity (Tato et al. 2005), and on the structural similarities with other RecA-like motor proteins that pump DNA between cellular foci or across membranes, such as FtsK or SpoIIIE (Cabezon et al. 2012). However, T4CPs are also essential for substrate translocation in the absence of DNA transfer (Draper et al. 2005; Jurik et al. 2010), and their ATPase activity is also required for relaxase translocation (de Paz et al. 2010).

In a previous work, we mapped functional domains of TrwB by *in vivo* analysis of a collection of TrwB variants (de Paz et al. 2010) and we identified a region, including the cytoplasmic entrance and surface of the ICH of the TrwB hexamer, involved in substrate transfer. In order to clarify the role of the ICH of the TrwB hexamer in conjugation, we have

addressed an *in vivo* and *in vitro* analysis of TrwB variants on residues at both ends and embedded into the ICH. The results obtained in this work support a model in which the ICH of the T4CP controls translocation of both DNA and protein substrates.

Materials and Methods

Bacterial strains

E. coli strains DH5α (Grant et al. 1990) and D1210 (Sadler et al. 1980) were used for cloning procedures and plasmid maintenance. For mating assays, strains D1210, DH5α or HMS174 (Campbell et al. 1978) were used as donors and recipients, as indicated. Strain C41 (Miroux and Walker 1996) was used for overexpression under the control of the T7 promoter.

Plasmid constructions

Plasmids used in this work are listed in **Table 1**. Plasmids constructions made for this work are described in **Supplementary Table S1**. Plasmids were constructed using standard methodological techniques (Sambrook and Russell 2001). The spontaneous mutations obtained in *trwB* in plasmid pDEL045 were separated by restriction cloning as detailed in Table S1. Constructs harboring *oriT+trwC* to test DNA transfer in the absence of TrwA were obtained by cloning *oriT* in place of the *trwA* gene in plasmid pET29::*trwAC* (Table S1). Two plasmids were obtained with both orientations of the *oriT* with respect to *trwC*. Since this difference could affect *trwC* levels and transfer efficiency, both were tested in the presence of the R388 *trwC* mutant pSU1458 (Llosa et al. 1994) and shown to be mobilizable and to complement *trwC* mutations with the same efficiency (data not shown). Since the *PtrwA* promoter is located at positions 272- 300 of the *oriT*, we selected the construct with *PtrwA*

promoter facing opposite orientation of *trwC*, so that it does not affect its expression (pDEL017; Table 1).

Bacterial conjugation assays under TrwB limiting conditions

Mating assays under TrwB limiting conditions were performed as previously described (de Paz et al. 2010), but using donor cells in exponential phase instead of stationary phase. Under these conditions, TrwB steady-state levels were reproducible, as judged by Western blot (data not shown). Briefly, pHP139-derived plasmids expressing mutated *trwB* under the control of the lactose promoter were used for mobilization of a plasmid containing *oriT* plus *trwA* and *trwC* (pHP138) or *oriT* plus *trwC* (pDEL017) through the T4SS of plasmid pKM101 present in plasmid pKM101Δ*mob*. This plasmid is a SmaI deletion derivative of pKM101 devoid of the whole DNA transfer region of pKM101, so it only codes for the T4SS. Matings were carried out using as donor the *lacI*^{q} strain D1210 in the absence of Isopropyl β-D-1-thiogalactopyranoside (IPTG) (repressed conditions), or under induced conditions as follows: overnight cultures of donor strains were diluted 1/20 dilution and growth for 2 hours in the presence of 0.5 mM IPTG, and the matings were performed on LB agar plates supplemented with 0.5 mM IPTG.

Relaxase transport assay

Triparental matings were performed to check for TrwC transport in the absence of DNA as described previously (de Paz et al. 2010), with modifications further explained in the text. pHP139-derived plasmids containing *trwB* (wild-type or mutants) were introduced in donor cells (D1210) that also contain plasmid pKM101Δ*mob* coding for the pKM101 T4SS and the non-mobilizable plasmid containing *PtrwA-trwA-trwC* genes (plasmid pET29::*trwAC)*. None of the three plasmids present in the donor cell contained an *oriT*, so there is no conjugative DNA transfer from the donor. Donor cells were mated with a second

strain (DH5α) harboring a *trwC*-deficient R388 derivative (plasmid pSU1445 (Llosa et al. 1994)). TrwC transport into this second strain was detected by complementation of the *trwC* mutation and subsequent mobilization of pSU1445 into a third recipient strain (HMS174). Mating assays were carried out from the *lacI*^{q} strain D1210 under repressed or induced conditions as described in the previous section.

DNA and protein transfer results are shown as the frequency of transconjugants per donor cell, and represent the mean of 3-5 independent experiments.

Western blot

The amount of TrwB protein was estimated by Western blot of total protein extracts. Overnight cultures of *E. coli* cells harboring plasmids containing *trwB* (wild-type and mutants) under TrwB liming conditions were diluted 1/20 and cells were grown to an optical density (OD) of 0.6. When indicated, 0.5 mM IPTG was added and growth continued for 1 or 3 hours post induction. Cells were collected, centrifuged, resuspended in 1/10 volume of 2 x SDS-gel loading buffer (Sambrook & Russell, 2001) and stored at -20°C. Samples were boiled for 10 min prior to electrophoresis, and equivalent amounts of total protein were loaded per well. Proteins were transferred from the gel onto nitrocellulose filters. Anti-TrwB primary antibody (de Paz et al. 2010) and peroxidase-conjugated anti-rabbit secondary antibody (SIGMA) were used at 1:5,000 and 1 :10,000 dilutions, respectively, in 1 X TBST + 1.5% of blocking agent. Detection was performed with the Supersignal kit (Pierce), and bands were analyzed on a Bio-Rad ChemiDoc apparatus.

Protein purification

TrwBΔN70 and derivatives were purified as described previously (Tato et al. 2005). Protein TrwAh (TrwA with a C-terminal His-tag) was also purified as described (Tato et al. 2007).

211 ***Protein and DNA quantification***

212 Protein concentrations were determined using BCA Protein kit (Pierce). Double
213 stranded pUC8 (Vieira and Messing 1982) DNA was purified by using Qiagen midi Kit and
214 quantified in a NanoDrop (ND-1000 Thermo) spectrophotometer.

215 ***Electrophoretic mobility shift assay (EMSA)***

216 Nonspecific binding of TrwBΔN70 to supercoiled plasmid DNA was assayed by EMSA
217 as described (Moncalian et al. 1999). 200 ng of pUC8 DNA were incubated in binding buffer
218 (50 mM PIPES-NaOH pH 6.2, 0.1 mM EDTA, 100 mM NaCl, 2 mM $MgCl_2$, Glycerol 5 % (v/v),
219 PMSF 0.001%) with increasing concentrations of TrwBΔN70 monomer (5-15 μM), or BSA as
220 a negative control, in a final volume of 10 μl for 10 min at 37ºC. The reaction mix was then
221 loaded on 0.8% agarose gel stained with Sybr Safe DNA gel Stain (INVITROGEN) and run at
222 100 V for 2.5 h. The shift of DNA was visualized in a Gel-Doc apparatus at 30 minutes
223 intervals.

224 ***Affinity chromatography***

225 Protein interactions with TrwA were assayed as described (Llosa et al. 2003). Briefly,
226 GST-TrwBΔN75 fusion proteins were partially purified from the soluble fraction obtained
227 after cell lysis by mixing with glutathione-Sepharose resin (Pharmacia) overnight at 4ºC. The
228 resin was then washed extensively with 1X PBS to remove unbound proteins. 20 μg of
229 purified TrwAh or BSA as a negative control were added in buffer A (50 mM Tris, pH 7.6; 50
230 mM NaCl; 5 mM $MgCl_2$; BSA 1 g/ml) and incubated at room temperature for 1 h. Following
231 incubation, unbound TrwAh was removed via extensive washing with 1X PBS. Afterwards,
232 the resin was incubated for 20 minutes at room temperature with 30 mM glutathione, and
233 centrifuged to remove insoluble proteins. Bound proteins (TrwBΔN75-TrwAh) were
234 collected from the supernatant. The elution process was repeated twice. Protein

concentration was quantified and 30 μg from each sample were loaded on SDS polyacrilamide gels and stained with Coomassie brilliant blue.

ATP hydrolysis assays

ATP hydrolysis was quantified by a coupled enzyme assay as described previously (Tato et al. 2007). ATPase activity of TrwBΔN70 or derivatives was analyzed in the presence/absence of 5 μM ssDNA (M13mp18 viral single-stranded DNA or ϕx174 Virion DNA, both from New England Biolabs), 10μM supercoiled dsDNA (pUC8) or 0.2 μM TrwA (tetramer). TrwA was pre-incubated for 10 min at 37°C in ATPase assay mixture. The ATPase reaction mixture contained 150 μl of 50 mM Pipes-NaOH, pH 6.2, 75 mM NaCl, 10 mM MgCl, 10% glycerol, 0.5 mM phosphoenolpyruvate, 0.25 mM NADH, 60 μg/ml pyruvate kinase, 60 μg/ml lactate dehydrogenase (Roche Applied Science or Sigma Aldrich enzymatic mix) and 5 mM ATP (CALBIOCHEM). All reactions were initiated by the addition of 0.3 μM TrwBΔN70 monomer. ATPase activity was measured indirectly by decrease in NADH absorbance at 340 nm for 10 min at 37 °C in a UV-1603 spectrophotometer (Shimadzu). The ATPase activity was calculated as nmol of ATP hydrolyzed per minute per mg of protein.

Electrostatics of TrwB

For electrostatics analysis of TrwB and variants, the hexameric biological unit of TrwB was used as the initial structure to model the wild type (wt) and mutant complexes (Gomis-Rüth et al. 2001). K275A, K389A and K421A mutants were modelled using VMD (Humphrey et al. 1996). Hydrogens were added to the complexes using VMD and the protonation state of histidines was predicted with Propka (Li et al. 2005). Vacuum minimization was carried out for 2000 steps (time-step 1fs/step) with the conjugate gradient minimization algorithm as implemented in NAMD (Phillips et al. 2005) using the CHARMM forcefield (Mackerell et al. 2004). Electrostatic potentials were computed with the finite difference Poisson-

Boltzmann (FDPB) method (Warwicker and Watson 1982), implemented in Delphi (Li et al. 2012b). Atomic charges and radii were extracted from the CHARMM forcefield (Huang and MacKerell 2013). The dielectric constant of the protein interior and the solvent were set to four and 80, respectively (Huang and MacKerell 2013). The ion exclusion parameter was set to two and the ionic strength to 145 mM. Electrostatic calculations were carried out using a lattice with 1.7 grids per Å and a series of focusing runs of increasing percentage fill (perfil) was performed from 20% to 90%. Calculations were iterated until they reached convergence, defined as the point at which the final maximum energy change is less than 10-4kTe-1. Visualization of electrostatic surfaces was carried out with PyMOL Molecular Graphics System, Version 1.8 Schrödinger, LLC.

Results

Construction of TrwB variants

According to current models for bacterial conjugation, the hexameric form of TrwB pumps DNA out of the cell through its ICH (Cabezon et al. 2015). Thus, positively charged residues within the ICH might interact with the negatively charged DNA backbone to facilitate transfer of the conjugative substrate (TrwC-DNA) through the T4SS. A previous report mapping TrwB functional domains (de Paz et al. 2010) suggested that several lysine residues mapping in the ICH (K275, K398 and K421) are involved in the process. Some of the constructs used in this work were double mutants, leading to variants K398A R417S and K421A D425A. In order to refine the previous analysis, new plasmids were constructed coding separately for different TrwB variants. Also, a double variant K275A K398A was

constructed. **Figure 1** shows the residues altered by mutagenesis, including a representation of the expected effect on charge distribution when each lysine is replaced by an alanine. The steady-state levels of these new TrwB proteins were similar to those of the wt protein, according to Western blot analysis (**Supplementary Figure S1**).

During the construction of TrwB K275A (de Paz et al. 2010), a plasmid including two additional spontaneous mutations was obtained, rendering TrwB variant P237L K275A S441G. The S441 residue also maps to the ICH (Fig. 1), so we isolated the mutation and included this variant in our present analysis.

Effect of* trwB *mutations on DNA transfer

In a previous work, we developed a conjugation assay in which the amount of TrwB was the limiting factor for DNA transfer, improving the detection of TrwB variant phenotypes (de Paz et al. 2010). The assay is based on controlled expression of *trwB* from the lactose promoter, and transfer through the T4SS of plasmid pKM101, which can replace the R388 T4SS although with lower efficiency (Llosa et al. 2003). We have improved the assay conditions by using donor cells in exponential phase, to avoid fluctuations in the steady-state level of TrwB (not shown). The effect of *trwB* mutations on DNA transfer was tested in this system (**Table 2**, assay I). TrwB variants N271D and K275A, previously reported not to affect DNA transfer efficiency (de Paz et al. 2010), consistently showed lower conjugation frequencies under the new assays conditions, while the newly constructed variants K398A and K421A showed conjugation frequencies higher than wt (3 and 4 fold higher, respectively) , and variant K275A K398A behaved similarly to wt. The triple variant K275A P337L S441G showed a strong reduction in DNA transfer efficiency (Table 2, assay I). A separate analysis of each mutation revealed that the variant S441G was responsible for

the observed phenotype in this protein (Table 2, assay I). Notably, S441 residue is located within the ICH, close to the transmembrane region (Fig. 1).

R388 conjugation is approximately 5-logs less efficient in the absence of TrwA (Moncalián et al. 1997). TrwB is known to interact with TrwA, which enhances its ATPase activity (Tato et al. 2007). In order to detect conjugation in the absence of TrwA we used a mobilizable plasmid coding for *oriT*+*trwC* in place of the plasmid coding for *oriT*+*trwA*+*trwC*. The steady-state levels of TrwB variants in the absence of TrwA did not show any significant difference, as judged by Western blot (Supplementary Figure S1). The results of conjugation assays in the absence of TrwA (Table 2, assay II) showed in most cases undetectable levels of DNA transfer, as expected. Interestingly, variants K398A, K421A and K275A K398A could catalyze DNA transfer, especially K398A.

Effect of* trwB *mutations on relaxase transport

The R388 relaxase TrwC can be translocated into the recipient cell in the absence of DNA transfer; this transport is dependent on TrwB (Draper et al. 2005). We assayed DNA-independent TrwC translocation in the presence of controlled amount of TrwB or its variants in triparental matings with some modifications over the previously published assay (de Paz et al. 2010), as detailed in Experimental Procedures. The reason for this change was that a closer inspection of donor cells under previously assayed conditions showed that the plasmid DNA content was unstable. This instability could be controlled by using P*lac*-driven expression of *trwB* from a $lacI^q$ donor strain. **Supplementary Figure S2** compares plasmid DNA content of donors under previous and present assay conditions, confirming that the structure of the plasmids remained unchanged after the mating assays. Donors contain three plasmids: i) a plasmid expressing *trwB* (wt or mutants) from the P*lac* promoter, ii) a plasmid coding for *trwA* and *trwC,* and iii) a plasmid coding for the pKM101 T4SS. None of

329 the three plasmids is mobilizable, since none carries an *oriT*. Donors were mated with a
330 second strain containing a R388 *trwC*-deficient mutant, and a third strain used to select for
331 transconjugants of the R388 *trwC* mutant, which could only be transferred upon
332 translocation of the TrwC protein from the donor strain (Draper et al. 2005).
333 Under these assay conditions, we found a correlation between DNA transfer and TrwC
334 translocation in all cases (Table 2, assay III). TrwB K398A and K421A, affected in lysine
335 residues embedded in the ICH, exhibited protein translocation frequencies almost one log
336 higher than wt TrwB, while protein variant K275A K398A showed an intermediate
337 phenotype between that of single variants, as was the case for DNA transfer. N271D and
338 K275A variants affecting ICH residues close to the cytoplasmic entrance, showed a decrease
339 in TrwC translocation efficiency, and TrwB S441G was completely deficient for TrwC
340 translocation under tested conditions.
341 ***Effect of* trwB *mutations on ATPase activity***
342 TrwBΔN70 displays ATPase activity *in vitro*, strongly stimulated by the presence of
343 both DNA and TrwA (Tato et al. 2007). Using purified proteins, ATP hydrolysis rates were
344 measured for TrwBΔN70 variants in the presence of different inducers using a fixed
345 concentration of TrwBΔN70 (0.3 μM), as described (Tato et al. 2007). Optimal
346 concentrations of dsDNA and ssDNA were determined by measuring the ATPase activity in
347 the presence of increasing DNA concentrations. The lowest DNA concentration that
348 rendered maximal activity was selected for subsequent analyses. Absolute ATPase values for
349 each protein in the presence/absence of ssDNA, dsDNA, TrwA with a C-terminal His-tag
350 (TrwAh), or a combination of inducers, are shown in **Figure 2A**. All substrates stimulated
351 TrwBΔN70 ATPase activity; when TrwAh plus ssDNA or dsDNA were added, a synergistic
352 effect was observed, as previously reported.

353 With respect to TrwBΔN70 variants, the increase in basal ATP hydrolysis rates (Fig.
354 2A, light blue bars) compared to wt TrwBΔN70 was 1.2 (K275A); 3 (K421A); 4.7
355 (K275AK398A); and 18 (K398A); the difference was significant ($p<0.001$) for all variants,
356 particularly K398A (p value 2.4*E-11), with the exception of K275A which did not show a
357 significant difference. When TrwA was added to the reaction mixture (Fig. 2A, green bars),
358 similar values of ATP turnover were observed for K421A, K398A and K275A K398A proteins
359 compared with TrwBΔN70, while K275A showed significantly lower rates. It is also
360 interesting to compare the induction rates of each protein in the presence/absence of
361 TrwAh, as shown in **Figure 2B.** Regardless of the absolute values obtained, all TrwBΔN70
362 variants showed lower rates of induction in the presence of TrwAh. In particular, TrwBΔN70
363 K398A showed no significant increase in its ATPase rate in the presence of TrwAh (Fig. 2B).
364 Fig. 2A shows ATPase values when dsDNA (red bars) or ssDNA (blue bars) were
365 added to the reaction. Addition of either DNA substrate increased the ATPase activity for all
366 proteins, but to different extents. TrwBΔN70 K421A and K398A, affecting residues
367 embedded within the ICH, caused an increase in ATP hydrolysis of 2.3 and 10 times with
368 respect to TrwBΔN70 respectively. TrwBΔN70 K275A exhibited a lower ATP hydrolysis rate
369 than wt, while the double variant K275A K398A rendered an intermediate phenotype, with
370 ATPase values similar to wt. However, induction rates (Fig. 2B) for most variants were
371 similar in fold increase relative to their basal ATPase activity, with the exception of K275A,
372 which exhibited almost no ATPase activity in the presence of the DNA substrate.
373 When both TrwAh and DNA were added (Fig. 2A, yellow and dark blue bars), most
374 proteins showed a synergistic effect as the wt, rendering higher ATPase values than in the
375 presence of these substrates separately. In particular, TrwBΔN70 K275A showed a relevant
376 increase in the ATPase activity only in the presence of both inducers, TrwAh and DNA (40-

fold increase compared to the rates in the presence of DNA only). The notable exception was TrwBΔN70 K398A, which exhibited a reduced ATPase activity in the presence of both DNA substrates and TrwAh compared with its ATPase rate in the presence of DNA only, reaching levels that resembled those of wt TrwBΔN70. Interestingly, in summary the effects on ATPase rates of the variants are highly attenuated in the presence of both DNA and TrwA, i.e. the situation mimicking the *in vivo* scenario. This could explain the moderate effect of these mutations in the conjugation assays.

Effect of* trwB *mutations on interactions with relaxosomal components.

Interactions with TrwA were evaluated by affinity chromatography as described (Llosa et al. 2003). The soluble domains of TrwBΔN75 and variants K275A, K398A and K421A were fused to the C-terminus of GST. Fusion proteins were bound to glutathione-Sepharose resin and analyzed for specific retention of TrwAh. TrwBΔN75-TrwAh complexes were eluted from the resin. As shown in **Figure 3A**, TrwBΔN75 variants retained as much TrwAh as the wt protein. To evaluate the DNA binding activity of TrwB variants, we purified the soluble TrwBΔN70 derivatives and performed an EMSA assay with supercoiled DNA substrates, as described previously (Moncalian et al. 1999). We did not observe significant differences in DNA retardation among ICH variants or wt TrwBΔN75 under tested conditions (Fig. 3B).

Discussion

Conjugative coupling proteins are proposed to act as connectors between the relaxosome and the T4SS, and DNA pumping motors. While protein interactions with relaxosome and T4SS components, DNA binding, and ATPase activity have been thoroughly

400 reported for this kind of proteins, their specific involvement in DNA translocation has not
401 been settled so far. This situation prompted us to address a study of selected residues which
402 could be likely involved in substrate translocation. A previous work highlighted the
403 importance of ICH of the TrwB hexamer (de Paz et al. 2010). The results of this work confirm
404 the role of the residues protruding into the ICH in translocation of both protein and DNA,
405 suggesting a common mechanism for transport of both types of molecules.
406 To get insight into the role of ICH in conjugation, we constructed a set of TrwB single
407 variants affecting the ICH. Selected lysine residues were replaced by alanine, affecting the
408 charge distribution at the cytoplasmic entrance (K275A) or the inside (K398A, K421A) of the
409 ICH (Fig. 1B), and their effect was analyzed, both *in vitro* and *in vivo*. In addition, residue
410 changes at both ends of the channel (N271D and S441G) were also tested *in vivo*. Our
411 results from the analysis of TrwB ICH variants *in vitro* and *in vivo* are summarized in **Figure 4**.
412 Under current tested conditions, we observe a consistent correlation between DNA transfer
413 and TrwC translocation rates (Table 1, compare assays I and III). This is an important result
414 which indicates that TrwB requirements are similar for TrwC and DNA transfer. TrwB
415 belongs to a wide family of ring-shaped, hexameric ATPase motors that translocate both
416 nucleic acids and polypeptides through membranes (Cabezón et al. 2011). The mechanism
417 by which the chemical energy from ATP hydrolysis is coupled to DNA or protein
418 translocation remains unclear. Within its family, TrwB is unique since it acts on a
419 nucleoprotein complex, and thus it must accommodate both a polypeptide and a single-
420 stranded DNA for translocation. Since no residue of TrwB has been found to have a specific
421 effect on DNA transfer, it is plausible that TrwB applies the same mechanism to promote
422 first translocation of the TrwC polypeptide and then the covalently attached single-stranded
423 DNA. Variants affecting such mechanism would be impaired in both protein and protein-

DNA translocation.

Our results reveal that TrwB N271D and K275A variants, affecting residues located at the cytoplasmic entrance to the ICH, and variant S441G at the other end of the ICH, in contact with the TMD, were impaired in substrate transfer. Moreover, the latter was obtained spontaneously when constructing K275A, suggesting a compensatory effect and thus a concerted action. In agreement with this hypothesis, we have previously reported that plasmids encoding TrwB variants K136T and K275A are frequently isolated carrying an IS10 insertion in the promoter region of the *cat* gene (Gonzalez-Prieto et al. 2015); this insertion was proposed to lead to higher expression levels of CAT, which would be selected to compensate the lower metabolism of the cell harboring the plasmid. Both K136T and K275A show a deficiency in ATP hydrolysis ((Moncalian et al. 1999) and Fig 2). In the Sec mediated polypeptide export mechanism, the ATPase SecA regulates the opening of the SecY-channel. A SecA mutant unable to hydrolyze ATP would maintain the channel in an open conformation, while not being competent for substrate translocation, which proceeds by opening-closing cycles (Allen et al. 2016). Similarly, the TrwB K275A variant might form a constitutively open version of the ICH, which may have a toxic effect compensated by S441G closing the other end of the ICH.

Tight control of ICH opening may require a second control point at the TMD end of the ICH. T4CPs have been proposed to act as transducers of a mating signal from the T4SS to the cytoplasm (Lang et al. 2011). In this scenario, residues that contact the membrane, such as S441 (Gomis-Rüth et al. 2001), may play a sensor role for transducing the signal coming from the extracellular milieu upon contact with a recipient cell. The existence of two control points for Type IV secretion was previously suggested for *A. tumefaciens* VirB9/10 (Jakubowski et al. 2005; Banta et al. 2011). It is conceivable that not a single protein

448 component, but the whole T4SS complex, has to sense both the mating signal from the
449 outside and the substrate recruitment from the cytoplasm in order to be activated for
450 secretion.
451 Electrostatic potential calculation of the ICH shows three distinct segments (Figure
452 1B): a short hydrophobic region at the cytosolic side, followed by a highly electronegative
453 middle segment and an electropositive second half. Both K275A and N271D variants
454 increase the electronegativity of the channel entrance, and both show a similar in vivo
455 effect on the transfer rates. It can be observed how K275A converts the ICH into a two-
456 segment channel (Fig 1B), suggesting that the hydrophobic entry might play a role in
457 cytosolic substrate recruitment. On the other hand, K398A and K421A variants maintain the
458 three-segment ICH domain but extend the electronegative passage towards the membrane-
459 proximal half of the ICH domain. Hexameric DNA and RNA motors often contain positive
460 charges within their ICH which are proposed to interact with the negative phosphate
461 backbone of nucleic acids during translocation. In the P4 packaging ATPase, replacement of
462 the conserved lysine residue by alanine reduced RNA stimulation of ATP hydrolysis (Kainov
463 et al. 2006). In the case of the Phi29 DNA packaging motor, four lysine rings result in four
464 relaying transitional pauses during translocation (Zhao et al. 2013). Interestingly, the
465 mutation of one of the four lysines facing the ICH had no significant effect on DNA
466 translocation (Fang et al. 2012), resembling the mild phenotype of our single-lysine
467 substitutions in TrwB function *in vivo*. K398 and K421 in TrwB could similarly set the pace for
468 ssDNA transport. The longer segment of electronegative charge in K398A and K421A
469 variants (Fig. 1B) could prevent transitional pauses during translocation; in agreement with
470 this idea, we observe that variants K398A and K421A showed the highest conjugation
471 frequencies, as well as absolute ATPase values. The role of these residues cannot be solely

DNA transport, since their alteration also increases relaxase translocation in the absence of DNA transfer (Table 2, assay III). It has been proposed that protein translocation motors evolved from DNA translocation motors (Mulkidjanian et al. 2007), so the elements originally designed to translocate nucleic acids could have been adapted to the translocation of peptides.

TrwB has been shown to interact with TrwA, which enhances its ATPase activity. In the absence of TrwA, no DNA transfer was observed under our mating conditions. However, we detected significant DNA transfer rates when wt TrwB was substituted by TrwB K421A and especially K398A (Table 1, assay II); in the case of K398A, DNA transfer efficiency was at least two logs above the background. To our knowledge, this is the first report of a T4CP variant which bypasses the requirement of accessory nicking proteins. Interestingly, K398A high ATPase activity was not induced by TrwA (Fig.2). Together, these results support the idea that variant K398A mimics the effect that TrwA produces on TrwB. It is tempting to speculate that this residue couples conformational changes induced by TrwA-binding to substrate transfer. K398 would work as a ratchet clog to prevent backwards movement of the translocating polymer; substrate-bound TrwA would induce a conformational change in K398, liberating the clog for the next transition of the substrate. Similar Brownian ratchet mechanisms have been proposed for the translocation of DNA as well as peptides through bacterial membranes (Allen et al. 2016; Hepp and Maier 2016). Variant K398A would have lost its TrwA-controlled clogging activity, leading to unregulated ATPase activity and faster substrate transport. Interestingly, comparison of K275A K398A double variant with single variants (Figure 4) shows an intermediate effect in transfer efficiency, as expected for the sum of both individual effects, while maintaining the TrwA-independence phenotype conferred by K398A, both *in vivo* and *in vitro*.

Acknowledgements

We are grateful to Sandra Barral and Stephanie Siegmund (University of Columbia, NY) for assistance with statistical analysis and English editing of the manuscript, respectively.

Compliance with Ethical Standards

Funding: This work was supported by grants BIO2013-46414-P, BFU2016-78521-R and BFU2014-55534-C2-1-P from the Spanish Ministry of Economy and Competitiveness to ML, EC and FdlC respectively. GL acknowledges funding from NIH grants GM030518, S10OD012351 and S10OD021764. DL was a recipient of a predoctoral fellowship from CSIC (JAE-PRE). DLG-H and IM were recipients of predoctoral fellowships from the University of Cantabria.

Conflict of interest: All authors declare that they have no conflict of interest.

Ethical approval: This article does not contain any studies with human participants or animals performed by any of the authors.

References

Allen WJ, Corey RA, Oatley P, Sessions RB, Baldwin SA, Radford SE, Tuma R, Collinson I (2016) Two-way communication between SecY and SecA suggests a Brownian ratchet mechanism for protein translocation. Elife 5

Atmakuri K, Cascales E, Christie PJ (2004) Energetic components VirD4, VirB11 and VirB4 mediate early DNA transfer reactions required for bacterial type IV secretion. Mol Microbiol 54:1199-1211

Banta LM, Kerr JE, Cascales E, Giuliano ME, Bailey ME, McKay C, Chandran V, Waksman G, Christie PJ (2011) An Agrobacterium VirB10 mutation conferring a type IV secretion system gating defect. J Bacteriol 193:2566-2574

Bauer T, Rosch T, Itaya M, Graumann PL (2011) Localization pattern of conjugation machinery in a Gram-positive bacterium. J Bacteriol 193:6244-6256

Cabezon E, de la Cruz F (2006) TrwB: an F(1)-ATPase-like molecular motor involved in DNA transport during bacterial conjugation. Res Microbiol 157:299-305

Cabezon E, Lanza VF, Arechaga I (2012) Membrane-associated nanomotors for macromolecular transport. Curr Opin Biotechnol 23:537-544

Cabezón E, Lanza VF, Arechaga I (2011) Membrane-associated nanomotors for macromolecular transport. Curr Opin Biotechnol

Cabezon E, Ripoll-Rozada J, Pena A, de la Cruz F, Arechaga I (2015) Towards an integrated model of bacterial conjugation. FEMS Microbiol Rev 39:81-95

Cabezón E, Sastre JI, de la Cruz F (1997) Genetic evidence of a coupling role for the TraG protein family in bacterial conjugation. Mol Gen Genet 254:400-406

535 Campbell JL, Richardson CC, Studier FW (1978) Genetic recombination and
536 complementation between bacteriophage T7 and cloned fragments of T7 DNA. Proc
537 Natl Acad Sci U S A 75:2276-2280
538 Cascales E, Christie PJ (2004) *Agrobacterium* VirB10, an ATP energy sensor required for type
539 IV secretion. Proc Natl Acad Sci U S A 101:17228-17233
540 Chen Y, Zhang X, Manias D, Yeo HJ, Dunny GM, Christie PJ (2008) *Enterococcus faecalis* PcfC,
541 a Spatially-Localized Substrate Receptor for Type IV Secretion of the pCF10 Transfer
542 Intermediate. J Bacteriol
543 Christie PJ (2016) The Mosaic Type IV Secretion Systems. EcoSal Plus 7
544 de la Cruz F, Frost LS, Meyer RJ, Zechner EL (2010) Conjugative DNA metabolism in Gram-
545 negative bacteria. FEMS Microbiol Rev 34:18-40
546 de Paz HD, Larrea D, Zunzunegui S, Dehio C, de la Cruz F, Llosa M (2010) Functional
547 dissection of the conjugative coupling protein TrwB. J Bacteriol 192:2655-2669
548 Draper O, César CE, Machón C, de la Cruz F, Llosa M (2005) Site-specific recombinase and
549 integrase activities of a conjugative relaxase in recipient cells. Proc Natl Acad Sci U S
550 A 102:16385-16390
551 Fang H, Jing P, Haque F, Guo P (2012) Role of channel lysines and the "push through a one-
552 way valve" mechanism of the viral DNA packaging motor. Biophys J 102:127-135
553 Fernández-González E, de Paz HD, Alperi A, Agúndez L, Faustmann M, Sangari FJ, Dehio C,
554 Llosa M (2011) Transfer of R388 Derivatives by a Pathogenesis-Associated Type IV
555 Secretion System into both Bacteria and Human Cells. J Bacteriol 193:6257-6265
556 Gilmour MW, Gunton JE, Lawley TD, Taylor DE (2003) Interaction between the IncHI1
557 plasmid R27 coupling protein and type IV secretion system: TraG associates with the
558 coiled-coil mating pair formation protein TrhB. Mol Microbiol 49:105-116

559 Gomis-Rüth FX, Moncalián G, de la Cruz F, Coll M (2002) Conjugative plasmid protein TrwB,
560 an integral membrane type IV secretion system coupling protein. Detailed structural
561 features and mapping of the active site cleft. J Biol Chem 277:7556-7566.
562 Gomis-Rüth FX, Moncalián G, Pérez-Luque R, González A, Cabezón E, de la Cruz F, Coll M
563 (2001) The bacterial conjugation protein TrwB resembles ring helicases and F1-
564 ATPase. Nature 409:637-641.
565 Gonzalez-Prieto C, Agundez L, Llosa M (2015) Chloramphenicol Selection of IS10
566 Transposition in the cat Promoter Region of Widely Used Cloning Vectors. PLoS One
567 10:e0138615
568 Gonzalez-Rivera C, Bhatty M, Christie PJ (2016) Mechanism and Function of Type IV
569 Secretion During Infection of the Human Host. Microbiol Spectr 4
570 Grant SG, Jessee J, Bloom FR, Hanahan D (1990) Differential plasmid rescue from transgenic
571 mouse DNAs into *Escherichia coli* methylation-restriction mutants. Proc Natl Acad Sci
572 U S A 87:4645-4649
573 Guglielmini J, de la Cruz F, Rocha EP (2013) Evolution of Conjugation and Type IV Secretion
574 Systems. Mol Biol Evol 30:315-331
575 Hepp C, Maier B (2016) Kinetics of DNA uptake during transformation provide evidence for a
576 translocation ratchet mechanism. Proc Natl Acad Sci U S A 113:12467-12472
577 Hormaeche I, Alkorta I, Moro F, Valpuesta JM, Goñi FM, de la Cruz F (2002) Purification and
578 Properties of TrwB, a Hexameric, ATP-binding Integral Membrane Protein Essential
579 for R388 Plasmid Conjugation. J Biol Chem 277:46456-46462
580 Hormaeche I, Iloro I, Arrondo JL, Goni FM, de la Cruz F, Alkorta I (2004) Role of the
581 transmembrane domain in the stability of TrwB, an integral protein involved in
582 bacterial conjugation. J Biol Chem 279:10955-10961

583 Hormaeche I, Segura RL, Vecino AJ, Goni FM, de la Cruz F, Alkorta I (2006) The
584 transmembrane domain provides nucleotide binding specificity to the bacterial
585 conjugation protein TrwB. FEBS Lett 580:3075-3082
586 Huang J, MacKerell AD, Jr. (2013) CHARMM36 all-atom additive protein force field:
587 validation based on comparison to NMR data. J Comput Chem 34:2135-2145
588 Humphrey W, Dalke A, Schulten K (1996) VMD: visual molecular dynamics. J Mol Graph
589 14:33-38, 27-38
590 Jakubowski SJ, Cascales E, Krishnamoorthy V, Christie PJ (2005) *Agrobacterium tumefaciens*
591 VirB9, an Outer-Membrane-Associated Component of a Type IV Secretion System,
592 Regulates Substrate Selection and T-Pilus Biogenesis. J Bacteriol 187:3486-3495
593 Jurik A, Hausser E, Kutter S, Pattis I, Prassl S, Weiss E, Fischer W (2010) The coupling protein
594 Cagbeta and its interaction partner CagZ are required for type IV secretion of the
595 *Helicobacter pylori* CagA protein. Infect Immun 78:5244-5251
596 Kainov DE, Tuma R, Mancini EJ (2006) Hexameric molecular motors: P4 packaging ATPase
597 unravels the mechanism. Cell Mol Life Sci 63:1095-1105
598 Kerr JE, Christie PJ (2010) Evidence for VirB4-mediated dislocation of membrane-integrated
599 VirB2 pilin during biogenesis of the Agrobacterium VirB/VirD4 type IV secretion
600 system. J Bacteriol 192:4923-4934
601 Lai EM, Chesnokova O, Banta LM, Kado CI (2000a) Genetic and environmental factors
602 affecting T-pilin export and T-pilus biogenesis in relation to flagellation of
603 *Agrobacterium tumefaciens*. J Bacteriol 182:3705-3716.
604 Lang S, Kirchberger PC, Gruber CJ, Redzej A, Raffl S, Zellnig G, Zangger K, Zechner EL (2011)
605 An activation domain of plasmid R1 TraI protein delineates stages of gene transfer
606 initiation. Mol Microbiol 82:1071-1085

607 Larrea D, de Paz HD, Arechaga I, de la Cruz F, Llosa M (2013) Structural independence of
608 conjugative coupling protein TrwB from its Type IV secretion machinery. Plasmid
609 70:146-153
610 Lawley TD, Gilmour MW, Gunton JE, Standeven LJ, Taylor DE (2002) Functional and
611 mutational analysis of conjugative transfer region 1 (Tra1) from the IncHI1 plasmid
612 R27. J Bacteriol 184:2173-2180
613 Li F, Alvarez-Martinez C, Chen Y, Choi KJ, Yeo HJ, Christie PJ (2012a) Enterococcus faecalis
614 PrgJ, a VirB4-like ATPase, mediates pCF10 conjugative transfer through substrate
615 binding. J Bacteriol 194:4041-4051
616 Li H, Robertson AD, Jensen JH (2005) Very fast empirical prediction and rationalization of
617 protein pKa values. Proteins 61:704-721
618 Li L, Li C, Sarkar S, Zhang J, Witham S, Zhang Z, Wang L, Smith N, Petukh M, Alexov E (2012b)
619 DelPhi: a comprehensive suite for DelPhi software and associated resources. BMC
620 Biophys 5:9
621 Lu J, Wong JJ, Edwards RA, Manchak J, Frost LS, Glover JN (2008) Structural basis of specific
622 TraD-TraM recognition during F plasmid-mediated bacterial conjugation. Mol
623 Microbiol 70:89-99
624 Llosa M, Bolland S, Grandoso G, de la Cruz F (1994) Conjugation-independent, site-specific
625 recombination at the *oriT* of the IncW plasmid R388 mediated by TrwC [published
626 erratum appears in J Bacteriol 1994 Oct;176(20):6414]. J Bacteriol 176:3210-3217
627 Llosa M, de la Cruz F (2005) Bacterial conjugation: a potential tool for genomic engineering.
628 Res Microbiol 156:1-6
629 Llosa M, Gomis-Rüth F-X, Coll M, de la Cruz F (2002) Bacterial conjugation: a two-step
630 mechanism for DNA transport. Mol Microbiol 45:1-8

631 Llosa M, Zunzunegui S, de la Cruz F (2003) Conjugative coupling proteins interact with
632 cognate and heterologous VirB10-like proteins while exhibiting specificity for
633 cognate relaxosomes. Proc Natl Acad Sci U S A 100:10465-10470
634 Mackerell AD, Jr., Feig M, Brooks CL, 3rd (2004) Extending the treatment of backbone
635 energetics in protein force fields: limitations of gas-phase quantum mechanics in
636 reproducing protein conformational distributions in molecular dynamics simulations.
637 J Comput Chem 25:1400-1415
638 Matilla I, Alfonso C, Rivas G, Bolt EL, de la Cruz F, Cabezon E (2010) The conjugative DNA
639 translocase TrwB is a structure-specific DNA-binding protein. J Biol Chem 285:17537-
640 17544
641 Miroux B, Walker JE (1996) Over-production of proteins in Escherichia coli: mutant hosts
642 that allow synthesis of some membrane proteins and globular proteins at high levels.
643 J Mol Biol 260:289-298
644 Moncalian G, Cabezon E, Alkorta I, Valle M, Moro F, Valpuesta JM, Goni FM, de La Cruz F
645 (1999) Characterization of ATP and DNA binding activities of TrwB, the coupling
646 protein essential in plasmid R388 conjugation. J Biol Chem 274:36117-36124
647 Moncalian G, de la Cruz F (2004) DNA binding properties of protein TrwA, a possible
648 structural variant of the Arc repressor superfamily. Biochim Biophys Acta 1701:15-23
649 Moncalián G, Grandoso G, Llosa M, de la Cruz F (1997) *oriT*-processing and regulatory roles
650 of TrwA protein in plasmid R388 conjugation. J Mol Biol 270:188-200
651 Mulkidjanian AY, Makarova KS, Galperin MY, Koonin EV (2007) Inventing the dynamo
652 machine: the evolution of the F-type and V-type ATPases. Nat Rev Microbiol 5:892-
653 899

654 Pena A, Matilla I, Martin-Benito J, Valpuesta JM, Carrascosa JL, de la Cruz F, Cabezon E,
655 Arechaga I (2012) The hexameric structure of a conjugative VirB4 protein ATPase
656 provides new insights for a functional and phylogenetic relationship with DNA
657 translocases. J Biol Chem 287:39925-39932
658 Phillips JC, Braun R, Wang W, Gumbart J, Tajkhorshid E, Villa E, Chipot C, Skeel RD, Kale L,
659 Schulten K (2005) Scalable molecular dynamics with NAMD. J Comput Chem
660 26:1781-1802
661 Ripoll-Rozada J, Zunzunegui S, de la Cruz F, Arechaga I, Cabezon E (2013) Functional
662 interactions of VirB11 traffic ATPases with VirB4 and VirD4 molecular motors in type
663 IV secretion systems. J Bacteriol 195:4195-4201
664 Sadler JR, Tecklenburg M, Betz JL (1980) Plasmids containing many tandem copies of a
665 synthetic lactose operator. Gene 8:279-300
666 Sambrook J, Russell DW (2001) Molecular cloning : a laboratory manual, 3rd edn. Cold
667 Spring Harbor Laboratory Press, Cold Spring Harbor, N.Y.
668 Sastre JI, Cabezón E, de la Cruz F (1998) The carboxyl terminus of protein TraD adds
669 specificity and efficiency to F-plasmid conjugative transfer. J Bacteriol 180:6039-6042
670 Schröder G, Krause S, Zechner EL, Traxler B, Yeo HJ, Lurz R, Waksman G, Lanka E (2002)
671 TraG-like proteins of DNA transfer systems and of the *Helicobacter pylori* type IV
672 secretion system: inner membrane gate for exported substrates? J Bacteriol
673 184:2767-2779.
674 Schröder G, Schülein R, Quebatte M, Dehio C (2011) Conjugative DNA transfer into human
675 cells by the VirB/VirD4 type IV secretion system of the bacterial pathogen *Bartonella*
676 *henselae*. Proc Natl Acad Sci U S A

677 Segura RL, Aguila-Arcos S, Ugarte-Uribe B, Vecino AJ, de la Cruz F, Goni FM, Alkorta I (2014)
678 Subcellular location of the coupling protein TrwB and the role of its transmembrane
679 domain. Biochim Biophys Acta 1838:223-230
680 Tato I, Matilla I, Arechaga I, Zunzunegui S, de la Cruz F, Cabezon E (2007) The ATPase activity
681 of the DNA transporter TrwB is modulated by protein TrwA: implications for a
682 common assembly mechanism of DNA translocating motors. J Biol Chem 282:25569-
683 25576
684 Tato I, Zunzunegui S, de la Cruz F, Cabezón E (2005) TrwB, the coupling protein involved in
685 DNA transport during bacterial conjugation, is a DNA-dependent ATPase. Proc Natl
686 Acad Sci U S A 102:8156-8161
687 Thomas CM, Nielsen KM (2005) Mechanisms of, and barriers to, horizontal gene transfer
688 between bacteria. Nat Rev Microbiol 3:711-721
689 Vecino AJ, de la Arada I, Segura RL, Goni FM, de la Cruz F, Arrondo JL, Alkorta I (2011)
690 Membrane insertion stabilizes the structure of TrwB, the R388 conjugative plasmid
691 coupling protein. Biochim Biophys Acta 1808:1032-1039
692 Vecino AJ, Segura RL, Ugarte-Uribe B, Aguila S, Hormaeche I, de la Cruz F, Goni FM, Alkorta I
693 (2010) Reconstitution in liposome bilayers enhances nucleotide binding affinity and
694 ATP-specificity of TrwB conjugative coupling protein. Biochim Biophys Acta
695 1798:2160-2169
696 Vieira J, Messing J (1982) The pUC plasmids, an M13mp7-derived system for insertion
697 mutagenesis and sequencing with synthetic universal primers. Gene 19:259-268
698 Wallden K, Williams R, Yan J, Lian PW, Wang L, Thalassinos K, Orlova EV, Waksman G (2012)
699 Structure of the VirB4 ATPase, alone and bound to the core complex of a type IV
700 secretion system. Proc Natl Acad Sci U S A 109:11348-11353

Warwicker J, Watson HC (1982) Calculation of the electric potential in the active site cleft due to alpha-helix dipoles. J Mol Biol 157:671-679

Whitaker N, Berry TM, Rosenthal N, Gordon JE, Gonzalez-Rivera C, Sheehan KB, Truchan HK, VieBrock L, Newton IL, Carlyon JA, Christie PJ (2016) Chimeric Coupling Proteins Mediate Transfer of Heterologous Type IV Effectors through the Escherichia coli pKM101-Encoded Conjugation Machine. J Bacteriol 198:2701-2718

Whitaker N, Chen Y, Jakubowski SJ, Sarkar MK, Li F, Christie PJ (2015) The All-Alpha Domains of Coupling Proteins from the Agrobacterium tumefaciens VirB/VirD4 and Enterococcus faecalis pCF10-Encoded Type IV Secretion Systems Confer Specificity to Binding of Cognate DNA Substrates. J Bacteriol 197:2335-2349

Zhao Z, Khisamutdinov E, Schwartz C, Guo P (2013) Mechanism of one-way traffic of hexameric phi29 DNA packaging motor with four electropositive relaying layers facilitating antiparallel revolution. ACS Nano 7:4082-4092

Table 1. Plasmids

Description	Plasmid name	Source
Plasmids for DNA and relaxase transport assays		
a) *Expression of trwB variants*		
pSU19::*trwB*	pHP139	(de Paz et al. 2010)
pSU19::*trwB(N271D)*	pHP145	(de Paz et al. 2010)
pSU19::*trwB(K275A)*	pDEL009	(de Paz et al. 2010)
pSU19::*trwB(K398A)*	pHP171	This work (Table S1)
pSU19::*trwB(K275AK398A)*	pHP148	This work (Table S1)
pSU19::*trwB(K421A)*	pDEL002	This work (Table S1)
pSU19::*trwB(P237LK275AS441G)*	pDEL045	This work (Table S1)
pSU19::*trwB(P237LK275A)*	pDEL014	This work (Table S1)
pSU19::*trwB(S441G)*	pDEL015	This work (Table S1)
b) *Helper plasmids*		
pET29C::P*trwA-trwA-trwC*	pET29::*trwAC*	(Draper et al. 2005)
pET29c::P*trwA-oriT-trwA-trwC*	pHP138	(de Paz et al. 2010)
pET29c::*oriT-trwC*	pDEL017	This work (Table S1)
pKM101 Tra^{-} $T4SS^{+}$ (*)	pKM101Δ*mob*	(Draper et al. 2005)
R388::Tn5*tac*1 in *trwC*	pSU1445	(Llosa et al. 1994)
R388::Tn5*tac*1 in *trwC*	pSU1458	(Llosa et al. 1994)
Plasmids for protein overproduction		
a) Protein purification		
T7 Expression vector	pET3a	Novagen
T7 Expression vector	pET29c	Novagen
pET3a::*trwBΔN70*	pSU4637	(Moncalian et al. 1999)
pET29c::*trwBΔN70(K275A)*	pDEL013	This work (Table S1)
pET29c::*trwBΔN70(K398A)*	pHP173	This work (Table S1)
pET29c::*trwBΔN70(K275AK398A)*	pHP176	This work (Table S1)
pET3a::*trwBΔN70(K421A)*	pMEC10	This work (Table S1)
pET22::*trwA-HIS6*	pSU1547	(Moncalian and de la Cruz 2004)
b) GST fusions		
Vector for GST fusions	pGEX-3X	Pharmacia
pGEX-3X::*trwBΔN75*	pMTX501	(Llosa et al. 2003)
pGEX-3X::*trwBΔN75 (K275A)*	pDEL020	This work (Table S1)
pGEX-3X::*trwBΔN75 (K398A)*	pDEL008	This work (Table S1)
pGEX-3X::*trwBΔN75 (K421A)*	pDEL007	This work (Table S1)

(*) SmaI deletion derivative of pKM101, encoding only the T4SS of its conjugative apparatus.

Table 2. DNA transfer and relaxase transport mediated by TrwB protein variants

		Assay type		
		I	II	III
Plasmid	**TrwB variants**	**DNA transfer + TrwA**	**DNA transfer - TrwA**	**TrwC transport**
C-	-	$<1.7 \times 10^{-6}$	$<3.4 \times 10^{-6}$	$<4.8 \times 10^{-6}$
pHP139	Wt	3.3×10^{-1}	$<3.1 \times 10^{-6}$	2.5×10^{-4}
pHP145	N271D	2.8×10^{-2}	$<7.5 \times 10^{-6}$	7.6×10^{-6}
pDEL009	K275A	7.2×10^{-2}	$<2.6 \times 10^{-6}$	1.4×10^{-5}
pHP171	K398A	**1.0**	**3.5×10^{-4}**	**1.6×10^{-3}**
pDEL002	K421A	**1.4**	**6.7×10^{-6}**	**2.2×10^{-3}**
pDEL045	P237L K275A S441G	4.3×10^{-4}	nd	$<4.8 \times 10^{-7}$
pDEL014	P237L K275A	1.2×10^{-1}	nd	1.9×10^{-6}
pDEL015	S441G	5.0×10^{-3}	$<5.6 \times 10^{-6}$	$<4.1 \times 10^{-6}$
pHP148	K275A K398A	1.8×10^{-1}	**6.6×10^{-5}**	5.2×10^{-4}

Assays type I-II test DNA transfer under TrwB limiting conditions in the presence/absence of TrwA in the donor, respectively. Assay III tests relaxase transport in the absence of DNA transfer. All experiments were performed using D1210 as donor strain. Frequencies are expressed as number of transconjugants per donor. They are the mean of at least 3 independent assays. Frequencies >3-fold different with respect to the wt value are shown in boldface or gray boxes, to show increased or decreased frequencies, respectively.

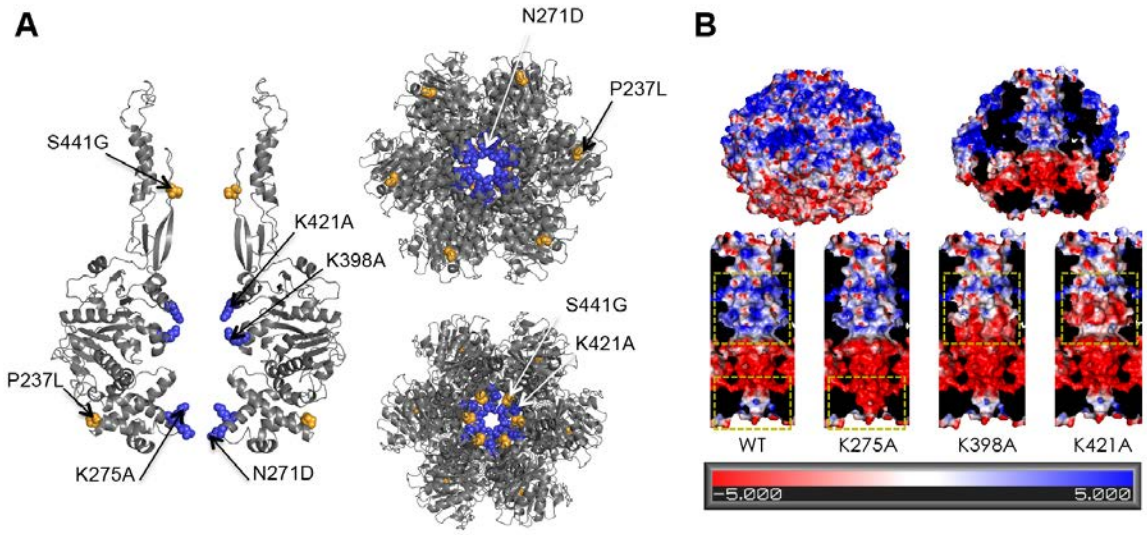

776

777 **Figure 1.** TrwB residues altered by mutagenesis. **A.** Ribbon representations of the 3D
778 structure of TrwB protein (membrane side on top, in all Figures) in which the TMD is
779 modeled as in (Gomis-Rüth et al. 2001). *On the left*, the figure shows the side view of two
780 opposing monomers where relevant residues are highlighted in red: Lysines protruding into
781 the ICH (K275; K398; K421), N271 in the entrance of the ICH. In green, P237 facing the
782 cytoplasm, and S441 protruding into the ICH close to the TMD. Amino acid changes made
783 for each residue are indicated by arrows. *Right top,* cytoplasmic view of the TrwB hexamer,
784 with the N271 asparagine ring closing the entrance to the ICH. *Right bottom,* membrane-
785 side view of the TrwB hexamer. **B.** Electrostatic potential of the wild type, K275A, K398A,
786 and K421A TrwB hexamers. *Top*, side views of the wild type TrwB hexamer, clipped on the
787 right to show the ICH. *Bottom*, close up views of the four ICH. Squares outline the regions
788 where the electrostatic potential changes in the different variants.

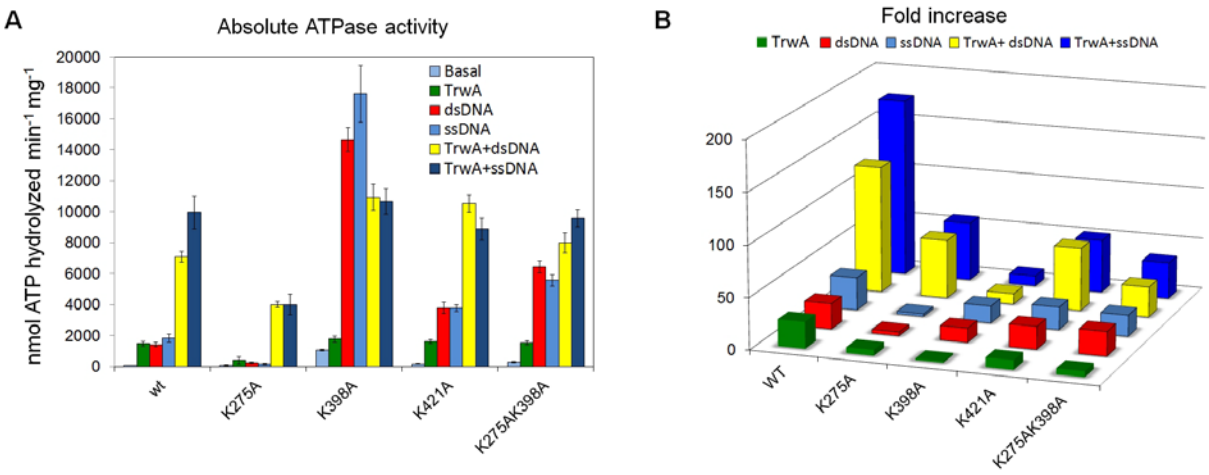

789

790 **Figure 2.** Effect of ATPase activity inductors TrwA and DNA on TrwBΔN70 and derivatives. **A.**
791 Absolute ATPase values. All reactions contained TrwBΔN70 or TrwBΔN70 variants (0.3 μM
792 as monomer), 5 mM ATP, 5 μM base ssDNA or 10 μM bp dsDNA, TrwAh (0.2 μM as
793 tetramer), or a combination of both substrates. Experiments were carried out with the
794 coupled spectrophotometric assay, initiating the reaction by the addition of TrwBΔN70
795 proteins. The effects of TrwA, dsDNA, ssDNA or TrwA+ DNA are shown in color code. For
796 comparison, basal ATPase activity has also been represented for each mutant. Data are
797 derived by averaging at least five experiments. **B**. ATPase activity plotted against the basal
798 activity. For each protein, the basal activity is considered as 1, to highlight the differences in
799 their increase in ATPase activity in the presence of DNA and/or TrwA.

800

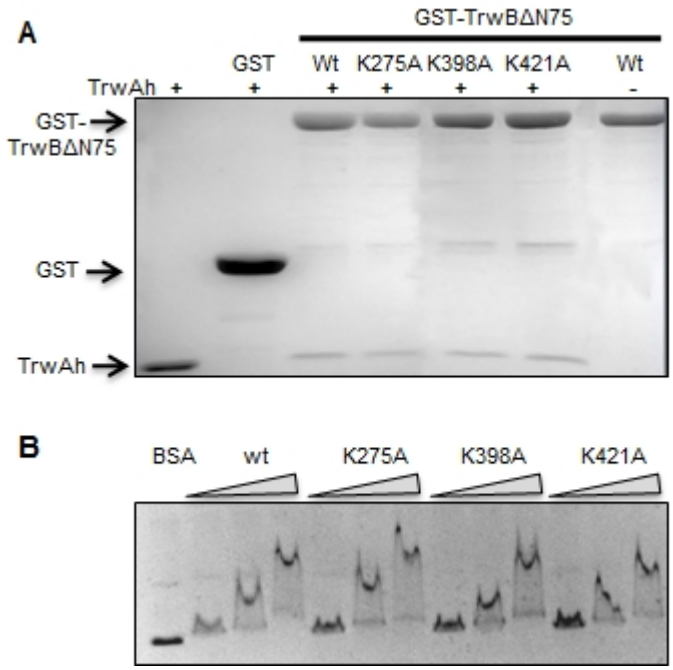

Figure 3. A. Protein–protein interactions detected by affinity chromatography. Soluble lysates containing GST-TrwBΔN75 fusion proteins were bound to glutathione-Sepharose resin, incubated with 20 μg of TrwAh or BSA and eluted with glutathione at 30mM. The figure shows 12% SDS-PAGE Coomassie-stained gels of eluted proteins (sizes indicated to the left with black arrows). GST: glutathione Sepharose transferase. GST-TrwBΔN75: fusion proteins containing the indicated residue changes. Incubation with TrwAh is indicated as - or + respectively. **B.** Electrophoretic mobility shift assay of TrwBΔN70 wt and variants. The DNA substrates were incubated at increased concentration (5, 10 and 15 μM of monomer) of the indicated proteins. The control in the first line was incubated with 15 μM of BSA.

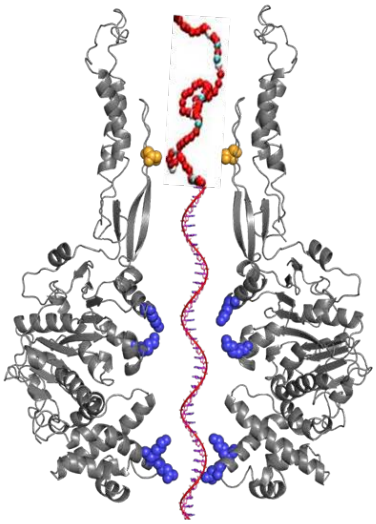

TrwB variant	In vivo transport			ATPase activity			
	DNA +TrwA	DNA -TrwA	TrwC +TrwA	Basal	-DNA +TrwA	+DNA -TrwA	+DNA +TrwA
Wild type	++++	-	+	(+)	+	+	++++
S441G	++	-	-	ND	ND	ND	ND
K421A	+++++	[[+]]	++	(+)	+	++	++++
K398A	+++++	+	++	+	+	+++++	++++
K275A K398A	++++	[+]	+	(+)	+	+++	++++
K275A	+++	-	[+]	(+)	(+)	(+)	++
N271D	+++	-	[[+]]	ND	ND	ND	ND

Figure 4. Summary of *in vivo* and *in vitro* phenotypes of TrwB or TrwBΔN70 derivatives with changes in residues protruding into the ICH. *Left*, representation of two opposing monomers of a TrwB hexamer, with relevant residues shown as in Fig.1. The unfolded TrwC polypeptide (bead string) and covalently attached single-stranded DNA are illustrated inside the ICH. *Right*, compilation of data taken from Table 1 (conjugation assays) and Fig. 2A (ATPase assays). The absolute values have been replaced by + symbols to facilitate comparisons. Data above or below wild type values are shown in green or red colors, respectively, to highlight the differences. Transfer frequencies (transconjugants per donor) are represented by +++++ (>10^{0}), ++++ (10^{-1}), +++ (10^{-2}), ++ (10^{-3}), + (10^{-4}), [+] (10^{-5}), [[+]](10^{-6}) and – (<10^{-6}). ATPase values (x μmol ATP hydrolyzed per min per mg) are represented by: +++++ (>12), ++++ (8-12), +++ (4-8), ++ (2-4), + (0.5-2), (+) (<0.5).